Macromolecules
ARTICLE

Macromolecules **2010**, *43*, 3897–3902 **3897**
DOI: 10.1021/ma100307m

FTIR Study on Hydrogen-Bonding Interactions in Biodegradable Polymer Blends of Poly(3-hydroxybutyrate) and Poly(4-vinylphenol)

Longhai Guo, Harumi Sato,* Takeji Hashimoto,† and Yukihiro Ozaki*

Department of Chemistry, School of Science and Technology and Research Center of Environmental Friendly Polymer, Kwansei-Gakuin University, Gakuen 2-1, Sanda 669-1337, Japan

Received February 8, 2010; Revised Manuscript Received March 16, 2010

ABSTRACT: The hydrogen-bonding interactions and the crystallinity of biodegradable polymer poly(3-hydroxybutyrate) (PHB) blended with poly(4-vinylphenol) (PVPh) were studied on the as-cast films as a function of the blend composition w_{PVPh} by using Fourier-transform infrared spectroscopy, differential scanning calorimetry, and wide-angle X-ray diffraction. The intermolecular hydrogen bondings between the C=O groups of PHB and the OH groups of PVPh (designated as *inter*) were explored not only in C=O stretching vibration region but also in OH stretching vibration region. The bands in OH stretching vibration region were assigned. The spectra in the C=O stretching vibration region were decomposed into component spectra attributed to *inter*, the free C=O groups, and the intramolecularly hydrogen-bonded C=O groups between the C=O groups and one of the C−H groups in CH_3 of PHB (designated as *free* and *intra*, respectively) to determine the respective fractions, f_{inter}, f_{free}, and f_{intra}. We found that f_ks (k = *intra* and *inter*) exhibit a double-step change with w_{PVPh}: (i) step 1 with $0 \leq w_{PVPh} \leq 0.5$, where *intra* and *inter* exchange each other, when w_{PVPh} is changed, via the two elemental transformations, (a) from *intra* to *free* and (b) from *free* to *inter*, as will be discussed in detail in the text; (ii) step 2 with $0.5 < w_{PVPh}$, where X-ray crystallinity tends to vanish, f_{free} starts to decrease, and f_{inter} starts to increase even more largely with w_{PVPh} than the case of (i), implying that the exchange from *free* to *inter* is suppressed by the presence of the crystallinity in step 1, while that from *free* to *inter* is enhanced in the absence of the crystallinity in step 2.

Introduction

Polyhydroxyalkanoates (PHAs) are well-known as naturally made biodegradable high molecular weight aliphatic polyesters that have the potential contributions to the environmental protection.[1−4] Among PHAs, poly(3-hydroxybutyrate) (PHB) is the most abundant polyester found in bacteria and also most extensively studied.[1,3] However, there is still a large technical barrier for practical applications of PHB as environmental-friendly polymeric materials because PHB is rigid and brittle due to its excessively high crystallinity, and it is also thermally unstable during the conventional melt-processing due to the high melting temperature (T_m).

The crystal structure of PHB is orthorhombic, $P2_12_12_1$-D^4_2 with lattice parameters a = 5.76 Å, b = 13.20 Å, and c = 5.96 Å (fiber repeat distance).[5,6] The crystals have the intramolecular hydrogen bondings (C−H···O=C) (designated hereafter as *intra*) between the C=O groups in one helix and the CH_3 groups in the other helix along the *a*-axis.[7−10] Moreover, *intra* can stabilize the chain folding in the lamellar structure of PHB.[9]

There are some approaches to improve the properties of PHB-based polymeric materials, such as copolymerization[11−16] and blending. Many blends containing PHB have been studied, such as poly(vinyl alcohol),[17] poly(vinyl acetate),[18] poly(methyl acrylate),[19] and poly(ethylene oxide).[20,21] It is well-known that the enthalpic contribution to the free energy of mixing usually controls the miscibility of polymer blends because polymer blends have small translational (combinatorial) entropy of mixing. Hydrogen-bonding interactions, if there are, are considered to play a key role in the enthalpic contribution due to its diversity and strength. Many hydroxyl group containing polymers are reported as a good counter polymer to be mixed with polyesters because those blends have been found to form totally or partially miscible systems driven by the intermolecular hydrogen-bonding interactions.[13,22−24]

We would like to further advance our discussion along this line by one step deeper and point out that the exchange of the hydrogen bonding between the intermolecular one (between the C=O groups in the polyester and the OH groups in the counter polymer) (designated hereafter as *inter*) and *intra*, and vice versa, would give crucial effects on both crystallization and miscibility. In a more rigorous sense, this exchange between *intra* and *inter* involves two elemental transformation processes: that between *intra* and *free* and that between *free* and *inter* as well. Here "*free*" designates the free C=O groups. The *inter* is expected to influence the glass transition temperature (T_g), increment of heat capacity, crystallinity, and crystal lattice parameters of the blends as well.

In this research, poly(4-vinlphenol) (PVPh) was selected as the hydroxyl group containing polymer and blended with PHB. Figure 1 shows the chemical structures of PHB (A) and PVPh (B). PVPh is completely amorphous, while PHB is semicrystalline. Because of the existence of C=O and OH groups in the constituent polymer (A) and (B), respectively, the blend is possible to form *inter*. Let us briefly review the works reported on PHB/PVPh blends below.

Xing et al.[25] reported that this particular blend system is miscible at all compositions through the single T_g evaluated by DSC thermograms and that the negative values of the segmental interaction parameter determined from the equilibrium melting point depression support the miscibility and strong hydrogen-bonding interactions between PHB and PVPh. Iriondo et al.[24,26] reported existence of inter in PVPh blends with tactic and atactic

*To whom all correspondence should be addressed. E-mail: ozaki@kwansei.ac.jp.
† Professor Emeritus, Kyoto University, Kyoto 606-8501, Japan.

Published on Web 03/26/2010

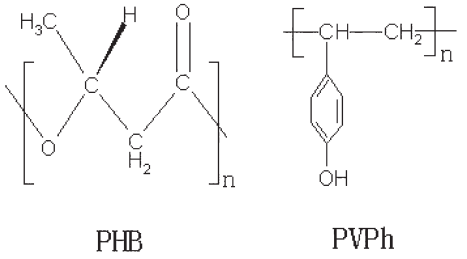

Figure 1. Chemical structures of poly(3-hydroxybutyrate) (PHB) (A) and poly(vinylphenol) (PVPh) (B).

PHB through the FTIR spectra in the C=O stretching vibration region. For the tactic PHB blends which are crystallizable, the specimens were heated above melting temperature, and the spectra were recorded in the cooling processes in order to avoid the influence of the crystallinity on the crystalline carbonyl band. Using the association model of Painter and Coleman,[27] they reported the difference in the equilibrium constants of the interassociation for the two blend systems with the tactic and atactic PHBs based upon the evaluated values of f_{inter} and f_{free} only under the conditions of $f_{intra} = 0$.

In this paper we aim to advance the investigation of this blend by one step further through systematically investigating the following parameters for the same samples: the thermal behavior with DSC, crystal structure, and crystallinity with wide-angle X-ray diffraction (WAXD), and *intra*, *free*, and *inter* with FTIR spectroscopy. The investigation was focused on the following aspects: (1) further reinforcement of existence of *inter* through the assignment of the OH stretching vibration bands in addition to the C=O stretching vibration bands; (2) decomposition of the vibration spectra in the C=O stretching region into fundamental vibration spectra reflecting *inter*, *intra*, and *free* in order to systematically study the transformations among them when w_{PVPh} is varied; (3) determination of X-ray crystallinity X_c and crystal lattice parameters. In item (2) described above, we should note that the decomposition process was generalized beyond the level of Iriondo et al.[24,26] and Gonzalez et al.[28] to include *intra* associated with crystallinity of the PHB phase.

Experimental Section

Materials and Sample Preparation Procedures. The bacterially synthesized poly(3-hydroxybutyrate) with number-averaged molecular weight $M_n = 6.5 \times 10^5$ was obtained from the Procter & Gamble Corp., Cincinnati, OH. Poly(4-vinylphenol), which is amorphous with glass transition temperature (T_g) equal to 118.2 °C and with weight-averaged molecular weight $M_w = 8.0 \times 10^3$, was provided by Aldrich Chemical Corp., Inc. PHB and PVPh were separately dissolved in chloroform and 2-butanone to prepare homogeneous solutions having concentrations 1 and 4 wt %, respectively. The two solutions were then mixed into a homogeneous solution and cast on CaF_2 substrates at 80 °C for 10 min. The cast films were kept in a vacuum oven at 60 °C for 24 h in order to evaporate the solvent completely and then cooled to room temperature. The samples thus prepared were designated hereafter as "as-prepared" samples and held in the vacuum oven at room temperature until measurements.

FTIR Spectroscopy. The transmission FTIR spectra were measured at 30 °C for the as-prepared samples of the PHB/PVPh blends using a Thermo Nicolet NEXUS 870 Fourier transform IR spectrometer (Waltham, MA) equipped with a liquid-nitrogen-cooled mercury−cadmium−telluride detector. A total of 256 scans were accumulated for signal-averaging of each IR spectral measurement to ensure a high signal-to-noise ratio with a 2 cm^{-1} resolution. The CN4400, OMEGA thermoelectric device (Boulder, CO) was used as a temperature controller with an accuracy ±0.1 °C.

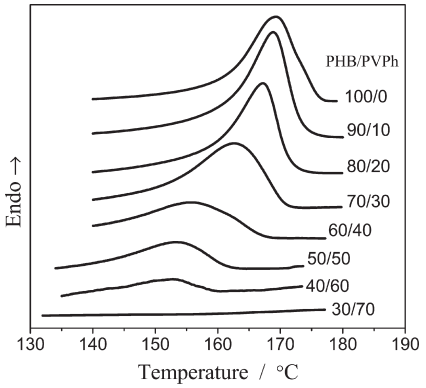

Figure 2. Melting endotherms of DSC thermograms recorded in the first heating process of the PHB/PVPh blends at 10 °C/min.

Differential Scanning Calorimetry (DSC). DSC measurements of PHB/PVPh blends were performed with a Perkin-Elmer Pyris6 DSC system (Waltham, MA) at heating and cooling rate of 10 K/min under a nitrogen purge. Separately from the as-prepared samples described above for FTIR measurements, the sample films for the DSC measurement were prepared by casting the solution on aluminum pans at 80 °C for 30 min and sealed in them. The samples were heated from 303 to 463 K (first heating process) and then maintained at 463 K for 2 min before cooling to 243 K. Subsequently, the samples were reheated to 463 K (second heating process). The value of the midpoint of the transition in the second heating process and peak point in the first heating process were taken as the T_g and T_m, respectively.

Wide-Angle X-ray Diffraction (WAXD). The WAXD patterns were measured for the as-prepared samples of PHB/PVPh blends at 30 °C in the scattering-angle range of $2\theta = 2°$—$40°$ by using Rigaku RINT2000 X-ray diffractometer (Tokyo, Japan) with Cu Kα radiation (wavelength 1.5418 Å) and with an X-ray generator of power 50 kV and 40 mA. The WAXD patterns of the blends were recorded as a function of w_{PVPh} at the scanning rate of $2\theta = 0.5°$/min at room temperature.

Results and Discussion

Thermal Analysis. Figure 2 shows the thermograms of the PHB/PVPh specimens during the first heating process. The temperature at the peak was taken as melting point (T_m). It is clear that, compared with pure PHB, the T_m and melting enthalpy of the blends decrease with w_{PVPh}, indicating that the blend system is miscible in the molten state and the crystallinity is depressed with w_{PVPh}, consistent with the results reported by Xing et al.[25] Moreover, the DSC curves of the blends with $w_{PVPh} \geq 70$ wt % do not exhibit the melting peak, indicating that the crystallization hardly occurs in these blends prepared as the above description. The disappearance of crystallinity will also be discussed in the following FTIR and WAXD parts.

Composition-Dependent FTIR Spectra in the C=O Stretching Region. Figure 3 shows the FTIR spectra obtained at room temperature for the as-prepared specimens of pure PHB and the PHB/PVPh blends with increasing w_{PVPh} in the C=O stretching vibration region. Two bands centered at 1742 and 1724 cm^{-1} are due to *free* and *intra*, respectively, each of which corresponds to the amorphous and crystalline states of PHB for the reasons as clarified below. For the spectrum with $w_{PVPh} = 90$ wt %, the peak around 1700 cm^{-1} (shown by the arrow) is due to a residual amount of the solvent (2-butanone) in the as-prepared films, which is difficult to be evaporated completely under the heat treatment employed in this work.

The composition-dependent FTIR spectra of the as-prepared specimens show the following trends with w_{PVPh}. The

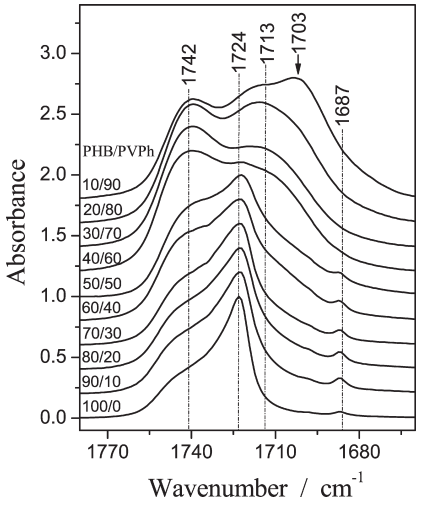

Figure 3. Normalized FTIR spectra recorded at room temperature in the C=O stretching region for the as-prepared PHB/PVPh blends.

sharp and dominant *intra* band around 1724 cm^{-1} gradually broadens and eventually disappears when $w_{PVPh} \geq$ 70 wt %, where crystallinity as observed by the melting exotherm disappears as shown in the DSC results (Figure 2). Besides, the absorption intensity of *free* around 1742 cm^{-1} increases with w_{PVPh}. Thus, we can reasonably assign *intra* and *free* to crystalline and amorphous bands, respectively. The second derivatives of the spectra in Figure 3 were calculated and shown in Figure 4. For the blend with w_{PVPh} = 70 wt %, the crystalline C=O band (or *intra*) totally disappeared. Moreover, this phenomenon can be verified also by the disappearance of a minor band centered at 1687 cm^{-1} when $w_{PVPh} \geq$ 70 wt %, as shown in Figures 3 and 4. This band has been reported to be undoubtedly a crystalline band, although its spectral origin is not yet assigned.[17] All of these suggest that PHB is no longer able to crystallize in the as-prepared PHB/PVPh blends when $w_{PVPh} \geq$ 70 wt %. This point will be further confirmed by the WAXD study to be discussed later.

Accompanied by the increased breadth of the band at 1724 cm^{-1} with w_{PVPh}, a new band appears at the lower wavenumber side around 1713 cm^{-1}, as shown in Figures 3 and 4. However, this peak exists neither in the pure PHB spectrum nor in the pure PVPh spectrum. Therefore, this is a new band inherent in the PHB/PVPh blend system and is expected to reflect *inter*. In general, the hydrogen bonding in the region from 1700 to 1720 cm^{-1} is quite well-known in many hydrogen-bonded polymer blends containing C=O groups and OH groups.[22,23] Actually, Iriondo et al.[24,26] also have reported existence of *inter* in the C=O stretching vibration region at ~1709 cm^{-1} for the PHB/PVPh blend specimens cooled down from the melts to 110 °C. They reported the contribution of *inter* increases with w_{PVPh}. Moreover, we found that the increase of *inter* with w_{PVPh} occurs in parallel to the decrease of *intra* and increase of *free*. These results ensure the formation of *inter*.

Intra stabilizes the chain folding in the lamella structure and hence brings about the high crystallinity of PHB.[9] On the other hand, the OH groups of PVPh hold the C=O groups of PHB from the amorphous phase through *inter*, so as to depress the crystallinity of PHB. With the increase of w_{PVPh}, *intra* appears to be exchanged into *inter*, which suppresses the crystallizability of PHB. Therefore, *intra* and *inter* can influence each other through the exchange between them, which will be discussed in the following part.

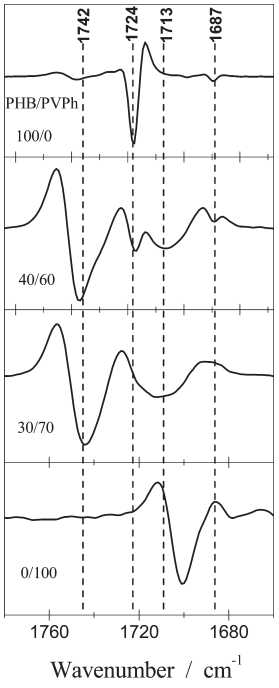

Figure 4. Second derivative of the spectra shown in Figure 3.

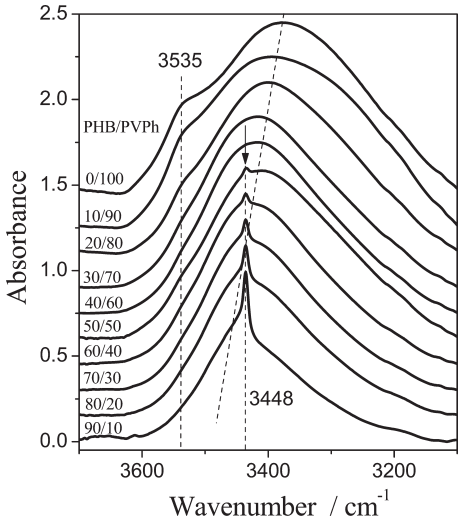

Figure 5. Normalized FTIR spectra recorded at room temperature in the OH stretching region for the as-prepared PHB/PVPh blends.

Composition-Dependent FTIR Spectra in the OH Stretching Region. Figure 5 shows the FTIR spectra in the OH stretching vibration region of pure PVPh and the PHB/PVPh blends with decreasing w_{PVPh} measured at room temperature. As shown in spectrum of pure PVPh, it exhibits two obvious stretching vibration bands, and we assign them due to the π-associated OH band around 3535 cm^{-1} and the self-associated OH band around 3380 cm^{-1}. The π-association is the interactions between the hydroxyl and phenyl groups of PVPh, and the self-association is the interactions among the OH groups of PVPh.

A narrow and sharp band centered around 3448 cm^{-1} observed in the FTIR spectra (shown by the broken line and the arrow) gradually decreases with w_{PVPh} and disappears when $w_{PVPh} \geq$ 60 wt %. The wavenumber of this band (3448 cm^{-1}) is the double of that of the crystalline C=O band (*intra* around 1724 cm^{-1}). Therefore, the band at 3448 cm^{-1} should

Table 1. Curve-Fitting Results of the C=O Stretching Vibration Bands in the PHB/PVPh Blends at Room Temperature

	free C=O (amorphous)			intra C=O (crystalline)			inter C=O (amorphous)		
PHB/PVPh (wt %)	ν^a (cm^{-1})	$w_{1/2}{}^b$ (cm^{-1})	fraction (%)	ν (cm^{-1})	$w_{1/2}$ (cm^{-1})	fraction (%)	ν (cm^{-1})	$w_{1/2}$ (cm^{-1})	fraction (%)
100/0	1739.5	25.07	51.3	1724.0	13.50	48.7			
90/10	1740.4	25.07	51	1724.0	13.50	34	1713.4	28.93	15
80/20	1740.4	25.07	49.8	1724.0	13.50	29.5	1713.4	28.93	20.7
70/30	1739.4	24.11	51.6	1723.1	13.50	24.4	1713.4	28.93	24
60/40	1740.4	24.11	51.8	1724.0	13.50	23.1	1712.5	28.93	25.1
50/50	1739.5	24.11	47.4	1722.1	12.54	24.1	1709.6	29.89	28.5
40/60	1741.4	24.11	49.8	1724.0	12.54	5	1713.4	30.86	45.2
30/70	1743.3	19.28	46				1716.3	41.46	52.5
20/80	1742.4	18.32	28.8				1715.4	42.43	71.2

[a] Peak wavenumber. [b] Full width at half-maximum.

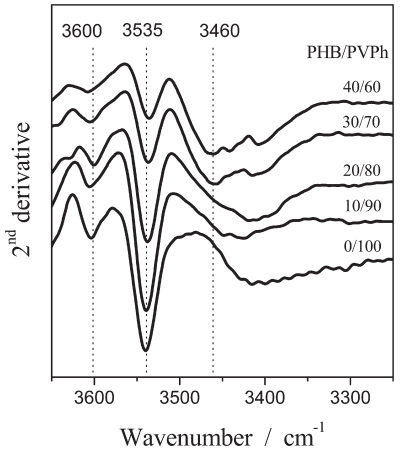

Figure 6. Second derivative of the spectra shown in Figure 5.

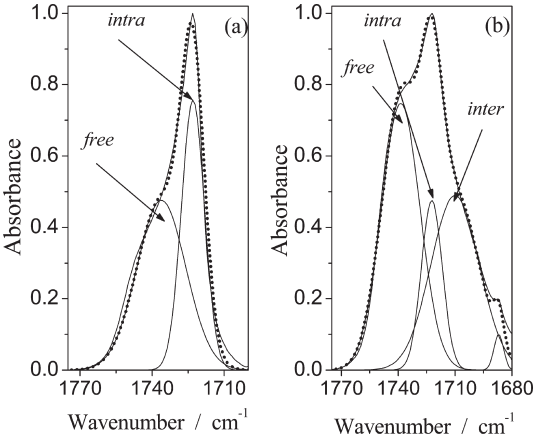

Figure 7. Decomposition of observed FTIR spectra in the C=O stretching region for neat PHB (a) and PHB/PVPh (wt %/wt %) = 50/50 (b) (solid line) into *free* (amorphous component), *intra* (crystalline component), and *inter* (amorphous component). The reconstructed absorbance (dotted line) was obtained by summing up of the absorbances of the elemental bands.

originate from the first overtone of the crystalline C=O stretching vibration at 1724 cm^{-1} of PHB. However, as shown in the C=O stretching vibration region (Figure 3), the *intra* C=O band disappears for the blends having $w_{PVPh} \geq$ 70 wt %. At w_{PVPh} = 60 wt %, the disappearance of the band around 3448 cm^{-1} is due to the low intensity of this band and the strong OH stretching vibration. This broad OH stretching vibration tends to cover the first overtone of the crystalline C=O band when the crystallinity is low. However, we can also detect the decrease of crystallinity of PHB through the intensity reduction of this first overtone band.

The second derivatives of the spectra in Figure 5 ($w_{PVPh} \geq$ 60 wt %), which were not affected by the first overtone of the crystalline C=O band, are shown in Figure 6. For pure PVPh spectrum, there is a peak around 3600 cm^{-1} which is not observed in original spectrum. The peak around 3600 cm^{-1}, which is barely visible in Figure 5, is reasonably assigned to the free OH groups of PVPh. We can clearly find another new band centered around 3460 cm^{-1} for the PHB/PVPh blends with w_{PVPh} = 60 wt %. Therefore, we propose that this new band is the *inter* OH band (OH···C=O) and combined with the self-associated OH band in the blend which is shifted from the neat PVPh band around 3380 cm^{-1} toward a higher wavenumber with the PHB content. This shift is in turn caused by *inter*. However, a quantitative assessment of the OH band in this region is quite difficult because of an extensive and intricate overlap of some bands.

Curve-Fitting Analysis for the Fraction of f_{free}, f_{intra}, and f_{inter}. The analysis of composition-dependent FTIR spectra in the C=O and OH stretching vibration regions confirmed the existence of *inter*. In order to quantitatively investigate the effect of composition on the individual elemental C=O stretching vibration bands around 1742 cm^{-1} (*free*), 1724 cm^{-1} (*intra*), and 1713 cm^{-1} (*inter*), a curve-fitting procedure was employed to decompose the net spectra in the C=O stretching region into the elemental vibrational bands. For the decomposition, each elemental spectrum was assumed to be Gaussian with the peak position determined from that of the second derivative of the spectrum. For instance, Figure 7 shows a typical curve-fitting result of the neat PHB (part a) and the PHB/PVPh (wt %/wt %) = 50/50 blend (part b). In the fitting process, the widths and heights of these peaks were treated as adjustable parameters. There is good agreement between the observed spectra (shown by the solid) and the reconstructed spectra (shown by the dotted line).

The fractions of *free*, *inter*, and *intra* respectively defined as f_{free}, f_{intra}, and f_{inter} were calculated on the basis of the Lambert−Beer law

$$f_k = (A_k/\varepsilon_k)/\sum_k (A_k/\varepsilon_k) \quad (1)$$

where A_k and ε_k are the absorbance and absorption coefficient of the elemental spectrum (k = *free*, *intra*, and *inter*). We used the reported value[23,24,26] of $\gamma \equiv \varepsilon_{inter}/\varepsilon_{free} = \varepsilon_{inter}/\varepsilon_{intra} = 1.5$ for the case of PVPh/polyester blend systems.

The results of the curve-fitting analysis are summarized in Table 2, and the fractions of each elemental vibration mode f_ks are shown as a function of w_{PVPh} in Figure 8. At a fist glance, it is striking to note that f_ks exhibit a double-step change with w_{PVPh} across $w_{PVPh} \sim$ 50 wt % as shown by the vertical broken line: step 1 at $w_{PVPh} <$ 50 wt % and step 2 at $w_{PVPh} >$ 50 wt % where crystallinity rapidly vanishes with w_{PVPh}. The first step involves a rapid increase of f_{inter} up to

Table 2. Degree of Crystallinity, Lattice Spacings, and Lattice Parameters of the As-Prepared PHB/PVPh Blends at 30 °C Determined from X-ray Diffraction

		lattice spacings[a]/Å			parameters of crystal lattice[a]/Å		
blend composition PHB/PVPh	crystallinity (%)	(020)	(110)	(002)	*a*	*b*	*c*
100/0	60 ± 5	6.57	5.25	2.92	5.72	13.14	5.85
90/10	58 ± 5	6.57	5.25	2.92	5.72	13.14	5.84
80/20	50 ± 5	6.53	5.22	2.91	5.70	13.06	5.82
70/30	47 ± 5	6.51	5.21	2.90	5.69	13.01	5.82
60/40	35 ± 5	6.52	5.21	2.91	5.69	13.05	5.83
50/50	29 ± 5	6.54	5.22		5.70	13.08	
40/60	9 ± 5	6.65	5.30		5.77	13.30	

[a] The errors in these values are ±0.01 Å.

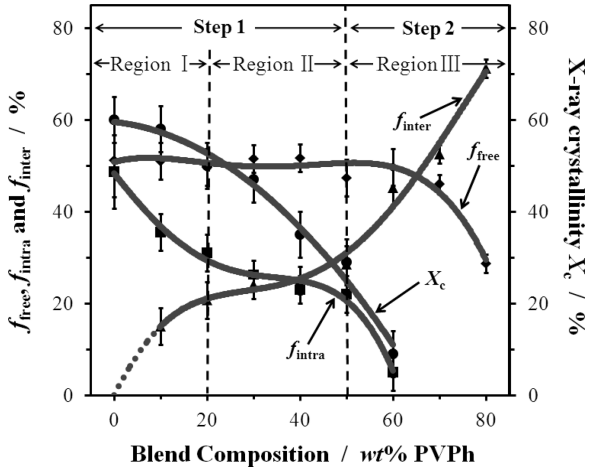

Figure 8. X-ray crystallinity (X_c) and fraction of *free* (amorphous), *intra* (crystalline), and *inter*. The solid lines are only for visual guides.

~20% as shown by the broken and solid line (the broken part was not actually measured but represents only an expected trend) (region I), followed by a small but almost linear increase of f_{inter} with increasing w_{PVPh} up to 50 wt % (region II). The second step (region III) involves another rapid sigmoidal increase of f_{inter} with w_{PVPh} by the amount which is even larger than that in the first step. The first-step increase of f_{inter} with w_{PVPh} occurs in parallel with a large and almost exponential decay of f_{intra} (region I), followed by a small but an almost linear decrease of f_{intra} (region II). The first-step rapid decay of f_{intra} is followed by an even more rapid parabolic decay (with an upward curvature at $w_{PVPh} \sim 50$ wt %) in the second step. Thus, both f_{intra} vs w_{PVPh} and f_{inter} vs w_{PVPh} have approximate inflection points at $w_{PVPh} \sim 20$ and 50 wt %. The changes in f_{intra} and f_{inter} suggest the exchange of the intra- and inter-molecular hydrogen bondings with the C=O groups of PHB. Moreover, the exchange behavior seems quite different below and above $w_{PVPh} \sim 50$ wt %. This "crossover behavior" will be further discussed later.

To our big surprise, f_{free} remains almost equal to that of neat PHB (~50 wt %) in step 1 compared with the large change of f_{intra} and f_{inter}. It then sharply drops with the further increase of w_{PVPh} in step 2, though the decrease begins to occur at ~60 wt % rather than at ~50 wt %. This disparity in the critical value of w_{PVPh}, above which f_{intra} and f_{free} start to decrease, will be briefly discussed later. The rapid decrease of f_{free} in the step 2 occurs concurrently with the sharp decrease of f_{intra}, hence with vanishing crystallinity and also with the large sigmoidal increase of f_{inter}. It is quite natural that the vanishing crystallinity as observed by the decrease of f_{intra} enhances the free C=O groups to contact with the OH groups of PVPh, so as to promote *inter* and suppress *free* in step 2.

The decrease of f_{intra} occurs essentially in parallel to the decrease of X-ray crystallinity X_c as shown in the right-side ordinate axis in Figure 8, as will be discussed in the next section. As already pointed out, in step 1, f_{free} remains almost unaltered with w_{PVPh}, in contrast to the large decrease of f_{intra} and hence X_c with w_{PVPh}. This evidence infers that the increased numbers of the free C=O groups created by the increased dissociation of *intra* in the crystalline region would not effectively encounter the OH groups of PVPh, because a majority of them are still stabilized and surrounded by the crystalline region. This may explain why f_{free} hardly changes with w_{PVPh}, despite the large decrease of f_{intra}.

The free C=O groups can easily encounter the OH groups of PVPh in step 2 because of the diminishing crystallinity, which in turn promotes the diffusion of the free C=O groups and hence the frequency factor for the association of *inter*. The disparity between the critical value of w_{PVPh} for *intra* (50 wt %) and that for *free* (60 wt %), above which f_{intra} and f_{inter} start to rapidly decrease with w_{PVPh}, is based on the same physics as described above. On one hand, the rapid decrease of f_{intra} in step 1 would bring about a large increase of f_{free} as a consequence of the dissociation of *intra*. On the other hand, the free C=O groups thus created can be more easily consumed and transformed into *inter* by the enhanced contacts with the OH groups of PVPh as PHBs are now essentially in amorphous phase. A balance of these two opposing effects is anticipated to result in the observed disparity in the critical value of w_{PVPh}. After all, these changes in f_{free}, f_{intra}, and f_{inter} suggest the exchange from *intra* to *inter* and vice versa occurs through *free* and that the degree of the exchange crucially depends on X_c of surrounding environment of free C=O groups.

In regions I and II of step 1, the addition of PVPh suppresses the crystallinity of PHB which in turn decreases f_{intra} and increases f_{free}. However, some of free C=O groups are associated with the OH groups of PVPh, so that f_{free} is kept unchanged, though f_{inter} increases. It should be noted that some of free C=O groups are trapped in amorphous region of PHB surrounded by the crystalline part and hence cannot be associated with the OH groups of PVPh. In region III, however, the crystalline region is totally destroyed, and hence the stabilization mechanism of free C=O groups disappears, so that the OH groups of PVPh can efficiently associate with the C=O groups of PHB to form inter. We found that there is a critical value of X_c (~30 wt %) or f_{intra} (~20 wt %) at $w_{PVPh} \sim 50$ wt % where a large change or the crossover occurs in the exchange efficiency.

Wide-Angle X-ray Diffraction Results. We measured the WAXD patterns of the as-prepared samples of the pure and blended PHB at 30 °C as a function of w_{PVPh}. The measured lattice spacings of the (020), (110), and (002) planes, crystallinity,

and the lattice parameters (*a*, *b*, and *c*) are show in Table 2. All the diffraction patterns of the blends have the same diffraction peaks as those of pure PHB, but the diffraction intensity decreases with w_{PVPh}. Therefore, the addition of PVPh does not result in any change of crystal structure of PHB, but it can depress the crystallinity of PHB in the blends. Moreover, as $w_{PVPh} > 50$ wt %, the diffraction peak intensity is so weak and hence the crystallinity is so low that the lattice parameter *c* could not be accurately measured. When $w_{PVPh} = 60$ wt %, the (020) and the (110) lattice spacings apparently increased, suggesting that the crystal lattices become less perfect, consistent with decreasing f_{intra} as clarified by the FTIR analysis. As $w_{PVPh} \geq 70$ wt %, the WAXD pattern shows the totally amorphous pattern without any diffraction peaks, indicating that the PHB component in these blends appears completely amorphous state. It is also consistent with the results of FTIR and DSC.

Figure 8 compares the crystallinity that were observed by WAXD (X_c) and FTIR (f_{intra}) as a function of w_{PVPh}. The observed trend that both X_c and f_{intra} decrease with w_{PVPh} is qualitatively the same but quantitatively different. The discrepancy may arise from a difference in the susceptibility of the two methods against thermal motions of the atomic groups: the break of intra, to which FTIR is sensitive, may not necessarily cause the degree of the distortion for the spatial order of atoms, to which X-ray diffraction intensity is sensitive.

Conclusions

The present studies have aimed at exploring the intra- and inter-molecular interactions, the crystal structure, and the crystallinity of the PHB/PVPh blends by using the combined FTIR, WAXD, and DSC methods. The following conclusions can be reached from the present study.

The intermolecular hydrogen bondings between the C=O groups of PHB and the OH groups of PVPh (*inter*) was further proven to exist, through the systematic assignment of the FTIR spectra in the OH stretching vibration region. Moreover, the competing hydrogen-bonding interactions of C=O groups in PHB with the CH_3 groups of PHB (*intra*) and with the OH groups of PVPh (*inter*) is a crucial physical factor underlying the basic physics of the blends with respect to ordering via crystallization, miscibility, and even phase separation, though the phase separation on this blend has not yet been critically investigated so far in the literature, especially during the ordering process prior to crystallization.

We proposed that the exchange between *intra* and *inter* occurs through creation of the free C=O groups (via dissociations of intra and/or inter), and hence it crucially depends on the mobility of the surrounding media where free C=O groups exist. This was evidenced by the crossover behavior of the exchange between *inter* and *intra* at the critical value $w_{PVPh} \sim 50$ wt % or at the critical value of crystallinity as observed by X-ray ($X_c \sim 30$ wt %) and FTIR ($f_{intra} \sim 20$ wt %).

WAXD studies of PHB/PVPh blends indicated that the crystal structure formed in the blends is same as that of neat PHB. Both of the X-ray crystallinity X_c and f_{intra} decrease with w_{PVPh}, although the trends of them are quantitively different as discussed in the text. The decreasing crystallinity of PHB/PVPh blends as a function of w_{PVPh} also was confirmed by the DSC thermograms.

We hope that our experimental results stimulate further fundamental studies to gain deeper insights into basic physics concerning the ordering process and mechanism of polymer blends in which both component polymers can form intra- and inter-molecular hydrogen bondings. To gain more profound understanding of the experimental results presented in this work, it is crucial to explore, in situ and at real time, the ordering process and mechanism (crystallization and/or phase separation) of the blends during the solvent evaporation process and the subsequent heat-treatment process.

Acknowledgment. This work was supported by Grant-in-Aid for Scientific Research (C) from MEXT (No. 20550026, No. 20550197), Grant-in-Aid for Scientific Research on Innovative Areas from MEXT (No. 21106521), and Shiseido Female Researcher Science Grant 2009. This works was supported also by Kwansei-Gakuin University "Special Research" project 2009−2014.

References and Notes

(1) Doi, Y. *Microbial Polyester*; VCH Publishers: New York, 1990.
(2) Anderson, A. J.; Dawes, E. A. *Microbiol. Rev.* **1990**, *54* (4), 450–472.
(3) Iwata, T.; Doi, Y. *Macromol. Chem. Phys.* **1999**, *200*, 2429–2442.
(4) Lara, M. L.; Gjalt, H. W. *Microbiol. Mol. Biol. Rev.* **1999**, *63* (1), 21–53.
(5) Cornibert, J.; Marchessault, R. H. *J. Mol. Biol.* **1972**, *71* (3), 735–756.
(6) Yokouchi, M.; Chatani, Y.; Tadokoro, H.; Teranishi, K.; Tani, H. *Polymer* **1973**, *14* (6), 267–272.
(7) Sato, H.; Murakami, R.; Padermshoke, A.; Hirose, F.; Senda, K.; Noda, I.; Ozaki, Y. *Macromolecules* **2004**, *37* (19), 7203–7213.
(8) Sato, H.; Dybal, J.; Murakami, R.; Noda, I.; Ozaki, Y. *J. Mol. Struct.* **2005**, *744−747*, 35–46.
(9) Sato, H.; Mori, K.; Murakami, R.; Ando, Y.; Takahashi, I.; Zhang, J.; Terauchi, H.; Hirose, F.; Senda, K.; Tashiro, K.; Noda, I.; Ozaki, Y. *Macromolecules* **2006**, *39* (4), 1525–1531.
(10) Sato, H.; Ando, Y.; Dybal, J.; Iwata, T.; Noda, I.; Ozaki, Y. *Macromolecules* **2008**, *41* (12), 4305–4312.
(11) Kunioka, M.; Nakamura, Y.; Doi, Y. *Polym. Commun.* **1988**, *29*, 174–176.
(12) Kunioka, M.; Tamaki, A.; Doi, Y. *Macromolecules* **1989**, *22* (2), 694–697.
(13) Xing, P.; Dong, L.; Feng, Z.; Feng, H. *Eur. Polym. J.* **1998**, *34* (8), 1207–1211.
(14) Sato, H.; Nakamura, M.; Padermshoke, A.; Yamaguchi, H.; Terauchi, H.; Ekgasit, S.; Noda, I.; Ozaki, Y. *Macromolecules* **2004**, *37* (10), 3763–3769.
(15) Sato, H.; Murakami, R.; Zhang, J.; Mori, K.; Takahashi, I.; Terauchi, H.; Noda, I.; Ozaki, Y. *Macromol. Symp.* **2005**, *230*, 158–166.
(16) Sato, H.; Murakami, R.; Zhang, J.; Ozaki, Y.; Mori, K.; Takahashi, I.; Terauchi, H.; Noda, I. *Macromol. Res.* **2006**, *14* (4), 408–415.
(17) Huang, H.; Hu, Y.; Zhang, J.; Sato, H.; Zhang, H.; Noda, I.; Ozaki, Y. *J. Phys. Chem. B.* **2005**, *109* (41), 19175–19183.
(18) An, Y.; Li, L.; Dong, L.; Mo, Z.; Feng, Z. *J. Polym. Sci., Part B* **1999**, *37* (5), 443−450.
(19) An, Y.; Dong, L.; Li, G.; Mo, Z.; Feng, Z. *J. Polym. Sci., Part B* **2000**, *38*, 1860−1867.
(20) Park, S. H.; Lim, S. T.; Shin, T. K.; Choi, H. J.; Jhon, M. S. *Polymer* **2001**, *42* (13), 5737–5742.
(21) Chee, M. J. K.; Ismail, J.; Kummerlowe, C.; Kammer, H. W. *Polymer* **2002**, *43* (4), 1235–1239.
(22) Moskala, E. J.; Howe, S. E.; Painter, P. C.; Coleman, M. M. *Macromolecules* **1984**, *17* (9), 1671–1678.
(23) Coleman, M. M.; Lichkus, A. M.; Painter, P. C. *Macromolecules* **1989**, *22* (2), 586–595.
(24) Iriondo, P.; Iruin, J. J.; Fernandez-Berridi, J. J. *Macromolecules* **1996**, *29* (17), 5605–5610.
(25) Xing, P.; Dong, L.; An, Y.; Feng, Z.; Avella, M.; Martuscelli, E. *Macromolecules* **1997**, *30* (9), 2726–2733.
(26) Iriondo, P.; Iruin, J. J.; Fernandez-Berridi, M. J. *Polymer* **1995**, *36* (16), 3235–3237.
(27) Coleman, M. M.; Graf, J. F.; Painter, P. C. *Specific Interactions and the Miscibility of Polymer Blends*; Technomic Publishing Co., Inc.: Lancaster, PA, 1991.
(28) Gonzalez, A.; Irusta, L.; Fernandez-Berridi, M. J.; Iriarte, M.; Iruin, J. J. *Polymer* **2004**, *45* (5), 1477–1483.